



P.23

(NASA-CR-190561) PERFORMANCE MEASUREMENT
RESULTS FOR A 220 Mbps QPPM OPTICAL
COMMUNICATION RECEIVER WITH AN EG/G SLIK APD
Interim Progress Report, 16 Oct. 1991 - 15
Jul. 1992 (JHU) 23 p

N92-29658

Unclas

G3/32 0109254

**ELECTRICAL
& COMPUTER
ENGINEERING**

**Performance Measurement Results for a
220 Mbps QPPM Optical Communication
Receiver with an EG&G Slik APD**

Frederic M. Davidson and Xiaoli Sun

Department of Electrical and Computer Engineering
The Johns Hopkins University, Baltimore, MD 21218

- Progress report on Grant NAG5-510
'Reduced electrical bandwidth receivers for direct detection
4-ary PPM optical communication intersatellite links'
for the period Oct. 16, 1991 to July 15, 1992.

July 1992

Performance Measurement Results for a 220 Mbps QPPM Optical Communication Receiver with an EG&G *Slik* APD

Frederic M. Davidson
Xiaoli Sun

Department of Electrical and Computer Engineering
The Johns Hopkins University
Baltimore, Maryland 21218

July 1992

1. Introduction

The performance was measured of a 220 Mbps quaternary pulse position modulation (QPPM) optical communication receiver [1] with a '*Slik*' silicon avalanche photodiode (APD) and a wideband transimpedance preamplifier in a small hybrid circuit module. The details of the QPPM encoder and receiver electronics are described in Reference [1]. The receiver performance had been poor due to the lack of a wideband and low noise transimpedance preamplifier. With the new APD preamplifier module, the receiver achieved a bit error rate (BER) of 10^{-6} at an average received input optical signal power of 4.2 nW, which corresponds to an average of 80 received (incident) signal photons per information bit.

2. Test Setup

The test setup is shown in Figure 1. The BER tester transmitter (Microwave Logic BERT-660Tx) generated pseudorandom binary sequences and served as a binary data source. The QPPM encoder converted every two bits into a PPM word which in turn modulated the laser transmitter. The optical signal was attenuated and photodetected by the silicon APD. The noise corrupted PPM sequences

output from APD preamplifier were subsequently processed and demodulated by the QPPM receiver. The BER tester receiver (Microwave Logic BERT-660Rx) compared the recovered binary sequences with the source binary data and determined the receiver BER.

The laser transmitter consisted of an AlGaAs laser diode (Mitsubishi ML5702A) operated at a wavelength of about 820nm. The laser diode driver and temperature control unit was made by NASA Goddard Space Flight Center. The laser diode was biased slightly below the threshold current (47mA) and the temperature was maintained at 25 °C. The average output optical power at the exit of the laser beam collimation lens was about 3.6 mW. Figure 2 shows the laser pulse shapes measured with a high speed photodiode (Opto-Electronics PD10). The photodiode had an inverting output due to its internal circuit configuration. The pulse rise and fall times from 10% to 90% pulse height were 330 and 500 ps, respectively. The average pulse width was about 2.1 ns. It was also found that pulsewidths varied by as much as 8.5% from one PPM word to another, which might have caused some degradation in receiver performance.

The propagation losses in free space were simulated by a set of neutral density attenuators. They were also used to adjust the input optical signal power to the receiver. The total attenuation of the attenuators was about 53 dB.

The receiver section of the optics consisted of a interference filter and a focusing lens. The interference filter was used to block out broad band laser diode noise and background radiation noise. The bandwidth of the filter at full width at half maximum (FWHM) was 9.0 nm and the peak transmission coefficient at the center wavelength was about 38%. The focusing lens was a 21X microscope objective lens with numerical aperture of 0.5.

3. *Slik* APD and Preamplifier Module

3.1. Description

Slik silicon APDs are state-of-the-art devices recently developed by EG&G Canada [2] which feature a 'super low ionization coefficients,' $k_{\text{eff}} \approx 0.005$ as compared to $k_{\text{eff}} \approx 0.020$ of the commercial grade devices. Typical quantum efficiency at 800 nm wavelength is about $\eta = 90\%$. The diameter of the active area of the APD is 100 μm . A hybrid circuit module was made by EG&G Canada which integrated a *Slik* APD with a lownoise and wideband (~ 1.0 GHz) transimpedance preamplifier (Anadigics ATA12000 [3]). The transimpedance of the preamplifier is 1.5 k Ω . The rated noise current density is about 5.0 pA/ $\sqrt{\text{Hz}}$ at 500 MHz and increases with frequency. The preamplifier also contains an automatic gain control (AGC) circuit although the AGC threshold current is relatively high (100 μA) as compared with our normal operation signal level (~ 0.5 μA at 5 nW input optical signal level). The APD high voltage bias supply consisted of a programmable DC to DC converter (Analog Modules 522-2). It had an internal temperature compensation circuit and the output ripple was 5 mV rms.

3.2. Test Results

The electrical characteristics of the APD preamplifier module (EG&G Canada C30964E CD1796, serial number 0011) were measured before use in the receiver. The bandwidth of the APD preamplifier module was determined by measuring the noise power spectrum of the APD preamplifier output while shining a relatively strong white light onto the APD active area. The APD was biased close to the breakdown voltage (-351 V). Two amplifiers (MiniCircuit ZFL1000-LN and ZFL1000, total gain 42dB) were used to further amplify the preamplifier output signal before being input to the spectrum analyzer. Figure 3 shows the measured spectrum. The 3dB bandwidth was found to be about 930 MHz.

The preamplifier noise current density was found by measuring the noise power spectrum while keeping the APD completely in the dark. The only noise sources under this condition were the APD dark current and the preamplifier circuit noise. The APD dark current noise was found so small that it caused little change in the noise spectrum when the APD bias voltage varied from well below to near the breakdown voltage. Figure 4 shows the measured noise power spectrum. At 200 MHz, the noise density was -112.8 dBm/Hz. Considering the 42 dB gain of the amplifiers, the noise power density at the preamplifier output was -155.8 dBm/Hz or 2.63×10^{-19} Watts/Hz. Multiplying it by 50Ω and taking the square root, the voltage noise density was $3.62 \text{ nV}/\sqrt{\text{Hz}}$. Dividing it by the transimpedance ($1.5 \text{ k}\Omega$), the current noise density was found to be $2.4 \text{ pA}/\sqrt{\text{Hz}}$. The spectral noise density measured at 800 MHz was roughly 8 dB greater than that at 200 MHz. Consequently, the current noise density at 800 MHz was $6.3 \text{ pA}/\sqrt{\text{Hz}}$. These measurement data agreed well with those given in the data sheet [3].

The APD ionization coefficient, k_{eff} , was found by measuring the APD output excess noise factor under a relatively strong CW incident laser light such that the APD excess noise became dominant. The APD excess noise factor, F , is defined as the ratio of the mean square to the square of mean of the APD gain and is related to the APD ionization coefficient by [4]

$$F = k_{\text{eff}}G + \left(2 - \frac{1}{G}\right) (1 - k_{\text{eff}}) \quad (1)$$

where G is the average APD gain. The excess noise factor is also the solution to the equation [5]

$$\frac{d\langle i^2 \rangle_{\text{ncw}}}{df} = 2qFG^2 \frac{\eta P_{\text{cw}}}{hf} \quad (2)$$

where $d\langle i^2 \rangle_{\text{ncw}}/df$ is the spectral noise current density, q is the electron charge, P_{cw} is the incident CW laser optical power, and hf is the photon energy.

The spectral noise current density was measured directly using a spectrum analyzer, similar to how the preamplifier noise current density was measured. The noise power spectral density was also measured with a RF power meter and a known bandwidth lowpass filter. The results were consistent with those measured with the spectrum analyzer. The incident CW laser optical powers were held at 50 nW and 100 nW, which were well below the preamplifier AGC threshold.

The average APD gain was determined by modulating the laser diode with a QPPM signal and measuring the pulse amplitude, V_{p-p} , of the output from the APD preamplifier. The average APD gain is the solution to the equation [5]

$$V_{p-p} = Gq \frac{\eta P_{p-p}}{hf} R_f A \quad (3)$$

where P_{p-p} is the peak-to-peak incident optical signal power, R_f is the preamplifier transimpedance, and A is the total gain of the amplifiers used after the preamplifier. The laser ON-OFF extinction ratio was kept high such that P_{p-p} was equal to the average optical signal power, P_{av} , divided by the PPM signal duty cycle, 25%. The average power was measured directly with an optical power meter. The APD gain was fixed at $G \approx 100$ during the measurements.

The APD ionization coefficient was obtained by substituting (3) and (2) into (1). The resultant ionization coefficient was $k_{eff}=0.02$. It is noted that the measured k_{eff} was four times greater than that of a *Slik* APD described in [2]. The discrepancy is yet to be explained.

Figure 5 shows the average pulse shape output from the APD preamplifier at 9.45 nW average input optical signal power. Pulseshape distortions due to the APD and the preamplifier are obvious when comparing Figure 5 to Figure 2.

4. Receiver Frontend

4.1. Amplifiers following the APD Preamplifier

Figure 6 shows a circuit diagram of the receiver frontend, which should supersede Figure 4 in Reference [1]. An AvanteK UTO511/505 cascade amplifier (5-500 MHz, 28 dB) was chosen as the first stage. The undershoot due to its relatively high lower cutoff frequency counteracted the residuals of pulse trailing edges at the bottom of the trace and consequently helped to reduce intersymbol interference caused by the residual. The signal was further amplified by another linear amplifier (MiniCircuit ZFL1000-LN, 0.1-1000 MHz, 23 dB). A variable attenuator was used between the two amplifiers to adjust the total gain. Figures 7 and 8 show the output signal waveforms. The signal was then split into the timing recovery circuit and the QPPM detection circuit.

4.2. Modification to the Timing Recovery Circuit

The original timing recovery circuit could tolerate only about 6 dB input signal dynamic range, which had caused great difficulties in optimizing the average APD gain and measuring the receiver BER vs. input optical signal power. The GaAs phase lock loop (PLL) chip (GigaBit Logic 16G040) for the PPM slot timing recovery was found to have too narrow an input signal dynamic range. We improved this by adding a high speed comparator as a limiter before the PLL chip. The detailed circuit diagram of the modified timing recovery circuit board is shown in Figure 9, which should supersede Figure 6 in Reference [1]. The original AvanteK GPD311/321 linear amplifier [1, p. 7] was also replaced with a wider dynamic range AvanteK GPD321/330 amplifier. The resultant dynamic range of the modified receiver increased to at least 20 dB as measured by connecting the QPPM encoder output directly to the receiver.

Two synchronization lock indicators were also added, one for the QPPM slot clock PLL and one for the QPPM word clock PLL. The output of the op-amp of the active loop filter of each PLL was first

buffered and then connected to a LED indicator. When a PLL was out of lock, the op-amp almost always drifted into saturation in one direction with a constant output voltage which turned on the LED indicator.

4.3. Raised Cosine Filter

An approximate raised cosine filter was installed in place of the original tapped delay line matched filter. The filter consisted of a linear amplifier (Avantek UTC2033) with a 20 pF shunt capacitor at the input, as shown in Figure 6. The input impedance of the amplifier and the shunt capacitor formed a lowpass filter which had a frequency response similar to a RC filter with a 3dB bandwidth of about 300MHz and a stopband (-20dB) of about 500 MHz. The attenuators at the input and the output of the linear amplifier were necessary to reduce the effect of impedance mismatching due to the added shunt capacitor. The output from the raised cosine filter was amplified again by a high power amplifier (Trontech P500A-3) to drive the subsequent QPPM detection circuit. Figure 10 shows the averaged waveform of the power amplifier output. The waveform looks similar to an ideal raised cosine pulses (inverted).

It should be pointed out that the lowpass filter we constructed was probably not a very good approximation to a true raised cosine filter as described in [6]. The receiver performance is expected to improve if one uses a better approach such as a Bessel lowpass filter or a transverse (tapped delay line) lowpass filter with similar bandwidth.

5. Measurement Results

The receiver BER was measured as a function of the average input optical signal power and the results are presented in Table 1 and Figure 11. The receiver achieved a BER of 10^{-6} at an average input optical signal power of 4.2 nW (-53.8 dBm), which corresponded to 80 incident photons per information bit. The measured optimal average APD gain was $G=110$.

The theoretical performance of an ideal QPPM receiver with a perfect rectangular input pulse shape and a matched filter is also plotted in Figure 11. The parameter values used are listed in Table 2. The laser ON-OFF extinction was assumed high (300) since the laser was biased below the threshold current. The APD bulk and surface leakage currents were taken to be 1.0 pA and 15 nA, which were typical values for silicon APDs. The noise spectral density of the preamplifier was assumed to be constant over the entire bandwidth and equal to 5.1 pA/√Hz (1.5 KΩ feedback resistance at an equivalent noise temperature of 700°K).

The measured input optical signal power at BER≈10⁻⁶ was about 1.5 dB higher than that of an ideal QPPM receiver. Considering the losses (~0.5 dB) due to the use of a raised cosine filter and nonrectangular input pulse shape, the difference between the theoretical calculation and the measurement should have been about 1.0 dB. We believed that this difference is mainly caused by the intersymbol interference from the ringing and long trailing edges of the pulses output from the APD preamplifier. The calculated optimal average APD gain at BER≈10⁻⁶ was about 36% higher than the measured data. This also suggested the existence of significant intersymbol interferences.

6. Conclusions

We have tested the 220 Mbps QPPM receiver with the newly developed *Slik* APD and Anadigics ATA12000 preamplifier module. The receiver achieved a BER of 10⁻⁶ at an average input optical signal power of 4.2 nW (-53.8 dBm), which corresponded to 80 incident photons per information bit. The test data are about 1 dB from the theoretically predicted performance.

The *Slik* APD we used had a measured ionization coefficient which was four times as large as what was promised [2]. In addition, the output of the APD preamplifier had significant ringing at pulse trailing edges and consequently caused intersymbol interference. The raised cosine filter was approximated with a simple lowpass

filter, which might also cause some degradation in receiver performance.

7. References

- [1] X. Sun and F. M. Davidson, 'Direct detection optical intersatellite link at 220 Mbps using AlGaAs laser diode and silicon APD with 4-ary PPM signaling,' Interim progress report on NASA grant NAG5-356, 'Optical communication with semiconductor laser diode' for the period Sept. - Feb. 1990, Dept. ECE, the Johns Hopkins University, Baltimore, MD 21218, March 1990.
- [2] A. D. MacGregor, B. Dion, and R. J. McIntyre 'High sensitivity, high data rate receivers for ISL using low-noise silicon APD's,' in *Optical Space Communication*, proc. SPIE, vol. 1131, Paris France, Apr. 24-26, 1989, pp. 176-186.
- [3] 'ATA12000 1.2 Gb/s AGC transimpedance amplifier,' Anadigics, Inc., 35 Technology Dr., Warren, NJ 07059 (phone 510-600-5741), Advanced product information, Rev. 1, May 1991.
- [4] P. P. Webb, 'Properties of avalanche photodiodes,' *RCA Rev.*, vol. 35, pp. 234-278, June 1974.
- [5] R. G. Smith and S. D. Personick, 'Receiver design for optical fiber communication system,' in *Semiconductor Devices for Optical Communication*, Springer-Verlag, New York, 1980, ch. 4.
- [6] F. M. Davidson and X. Sun, 'Bandwidth requirements for direct detection optical communication receivers with PPM signaling,' in *Free-Space Laser Communication Technologies III*, David L. Begley and Bernard D. Seery, Eds., proc. SPIE 1417, 1991, pp. 75-88.

Table 1.
Receiver BER vs. Average Input Optical Signal Power

Receiver BER	Average received Power (nW)	Average received photons/bit
3.1e-5	3.09	58.1
9.6e-6	3.44	64.7
2.7e-6	3.88	73.0
1.1e-6	4.15	78.1
1.0e-6	4.17	78.4
3.5e-7	4.30	80.9
8.0e-8	4.87	91.2
3.3e-8	5.43	102
1.0e-8	5.98	112

Table 2.
Parameter Values Used in the Theoretical Receiver Performance Calculations

binary source data rate	220 Mbps
QPPM pulsewidth	$\tau=(2 \times 220 \times 10^6)^{-1}$ s
laser diode wavelength	$\lambda=820$ nm
laser ON-OFF extinction ratio	300
APD quantum efficiency	$\eta=90\%$
APD surface leakage current	$I_s=15$ nA
APD bulk leakage current	$I_b=1.0$ pA
APD Ionization coefficient	$k_{eff}=0.020$
Preamplifier transimpedance	$R_f=1.5$ K Ω
equivalent noise temperature	$T_e=700$ °K (5.1 pA/ $\sqrt{\text{Hz}}$)

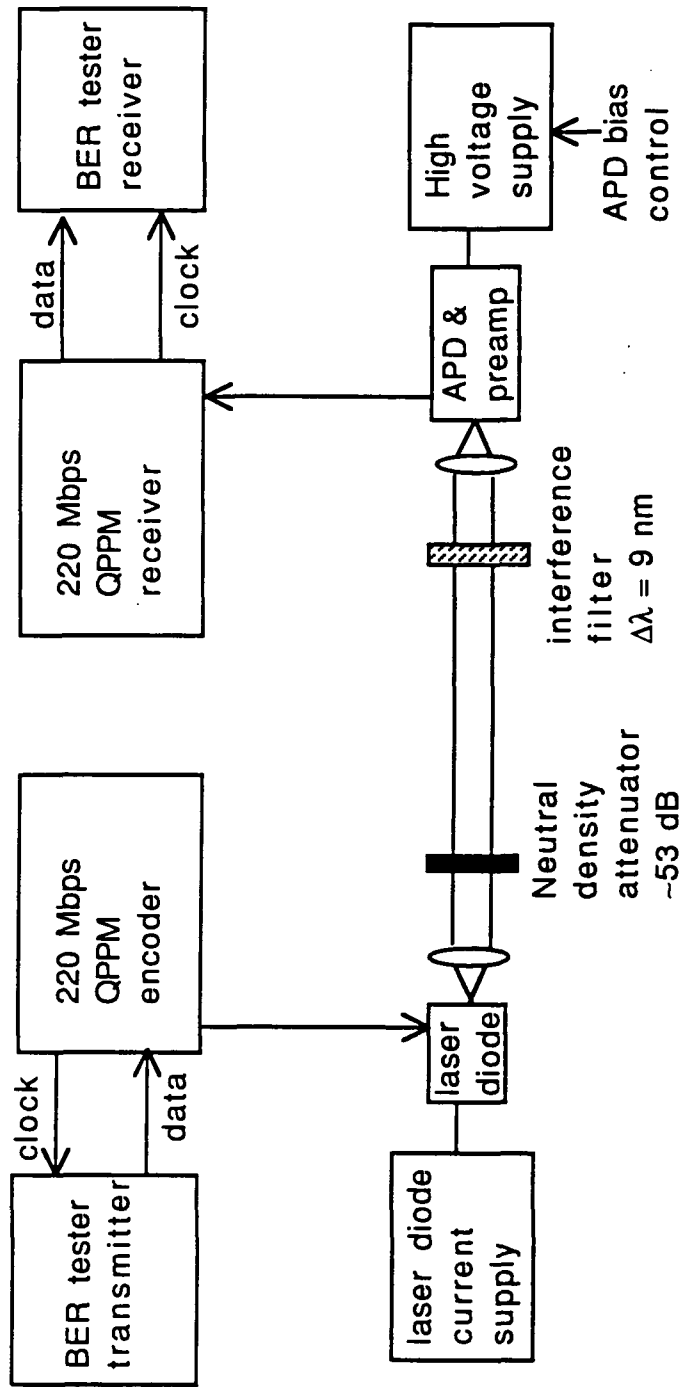
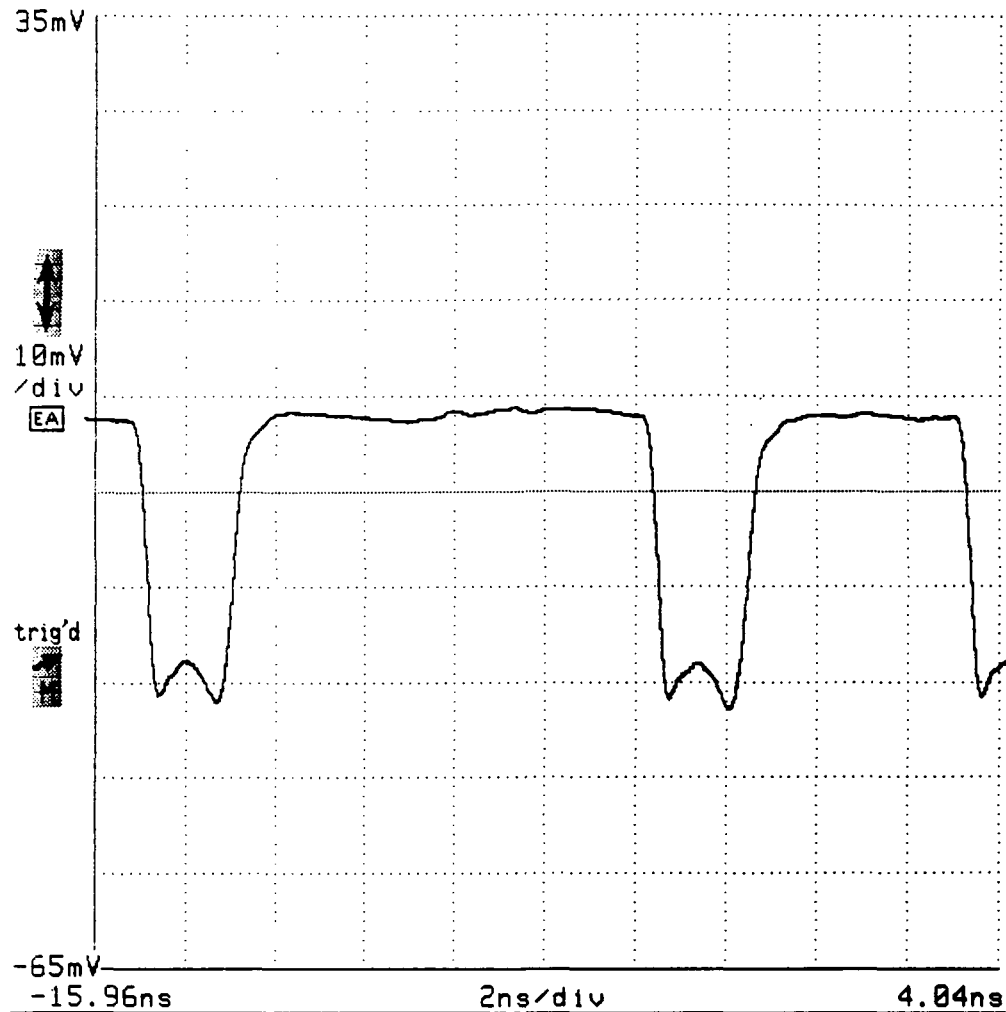


Figure 1. Block diagram of the test setup.

Tek



				0%
30.40 mV	1.932 ns	498.2 ps		43%
326.4 ps				Avg(C2) Main

Figure 2. Pulse shapes of the laser diode transmitter measured with a high speed photodiode (inverting output).

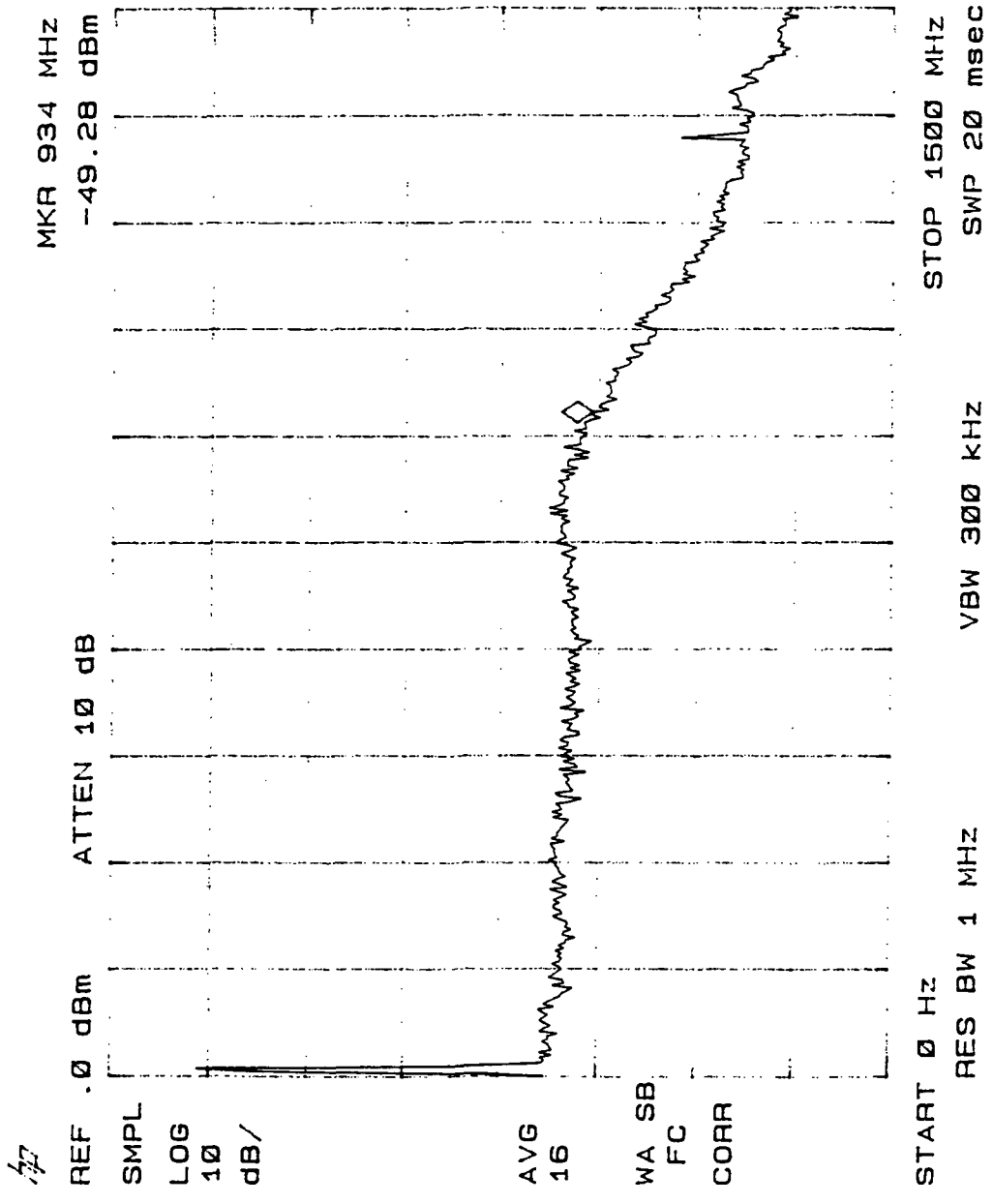


Figure 3. Frequency response of the APD preamplifier module measured with a spectrum analyzer while illuminating the APD with relatively strong white light.

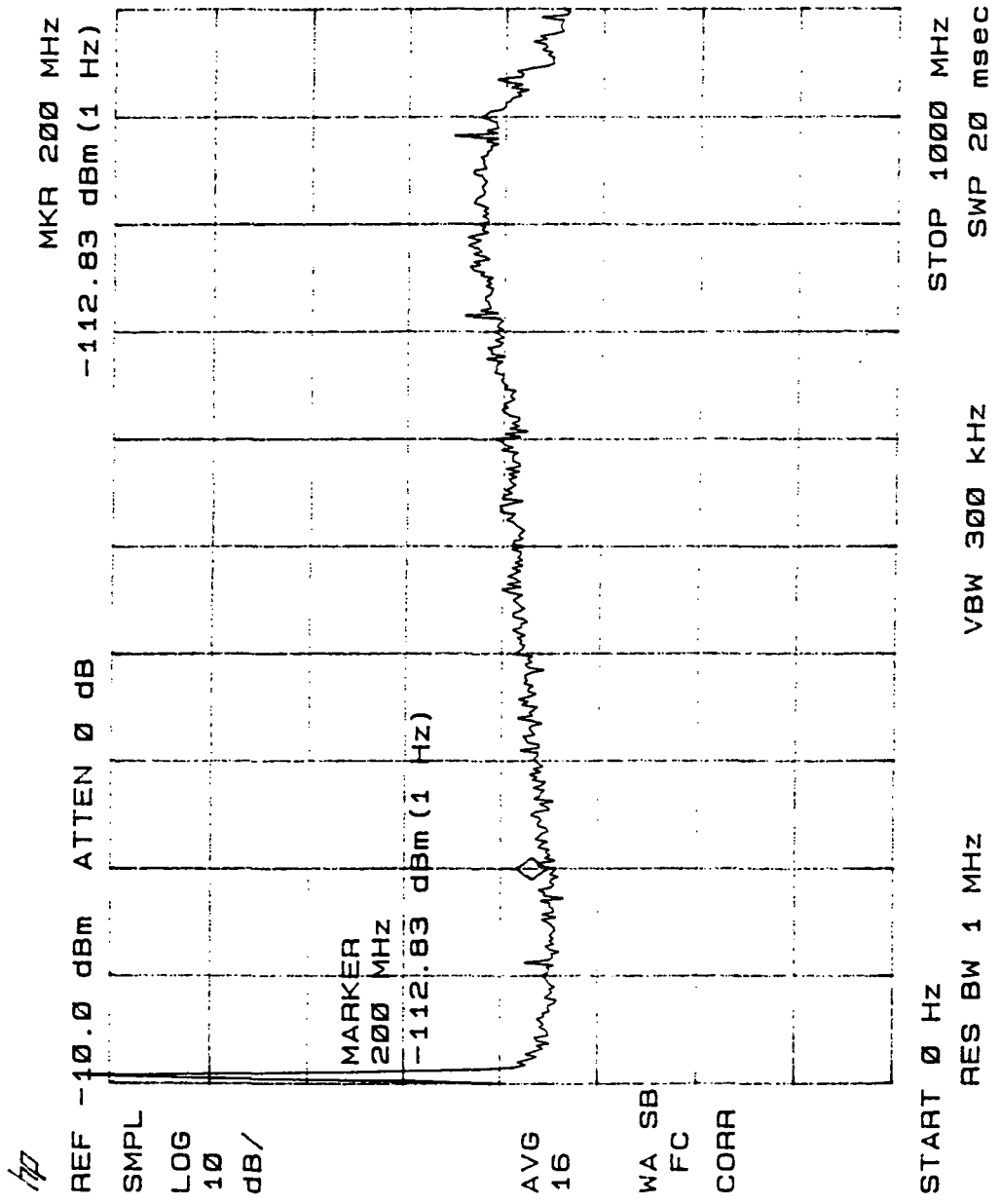
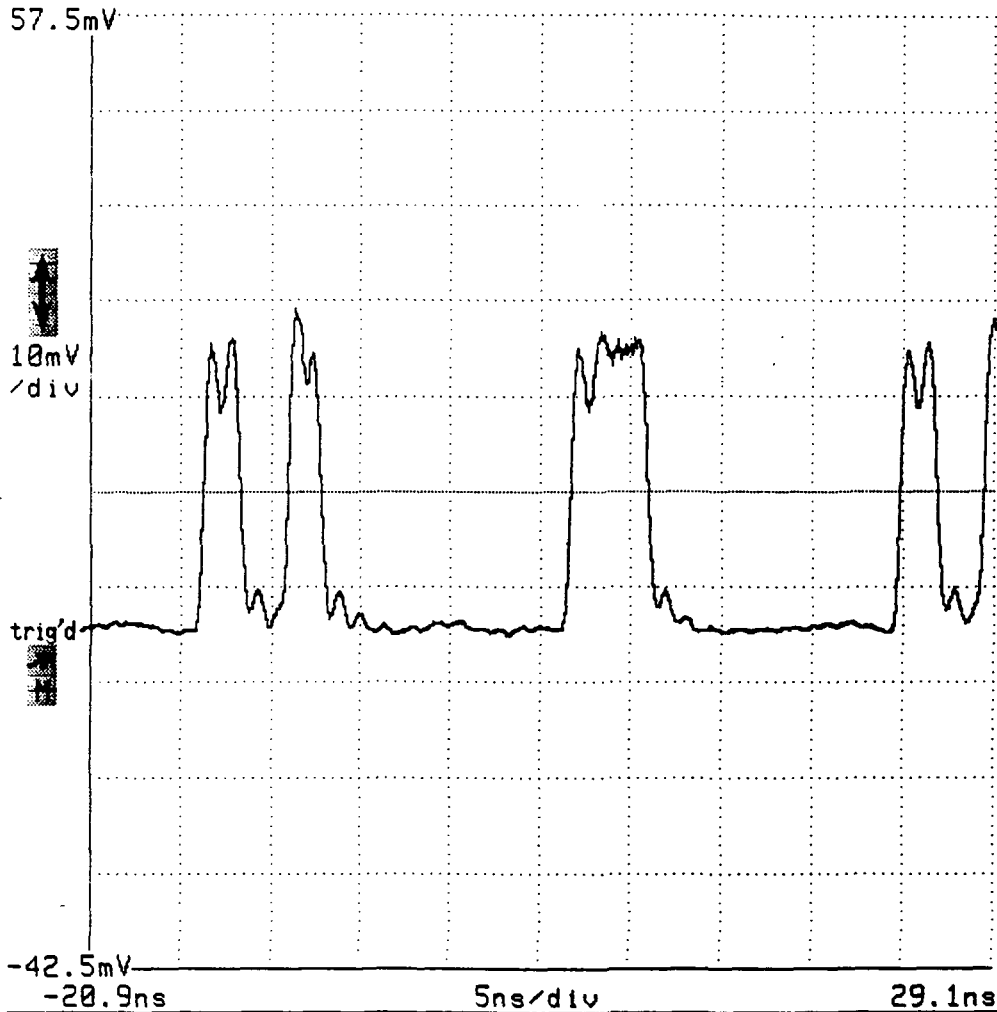


Figure 4. Dark noise power spectrum of the APD preamplifier module.

Tek



				5ns/div	
				29.1ns	
			5ns/div		
Avg(C1)	Main	Avg# >16	Linear		
Fast	@ 1024 pts			-21.5ns	
50Ω	AC	1GHz	All Wfms Status	Avg(C1) Main	off

Figure 5. Average output pulse shape from the APD preamplifier module at 9.45 nW average input optical signal power.

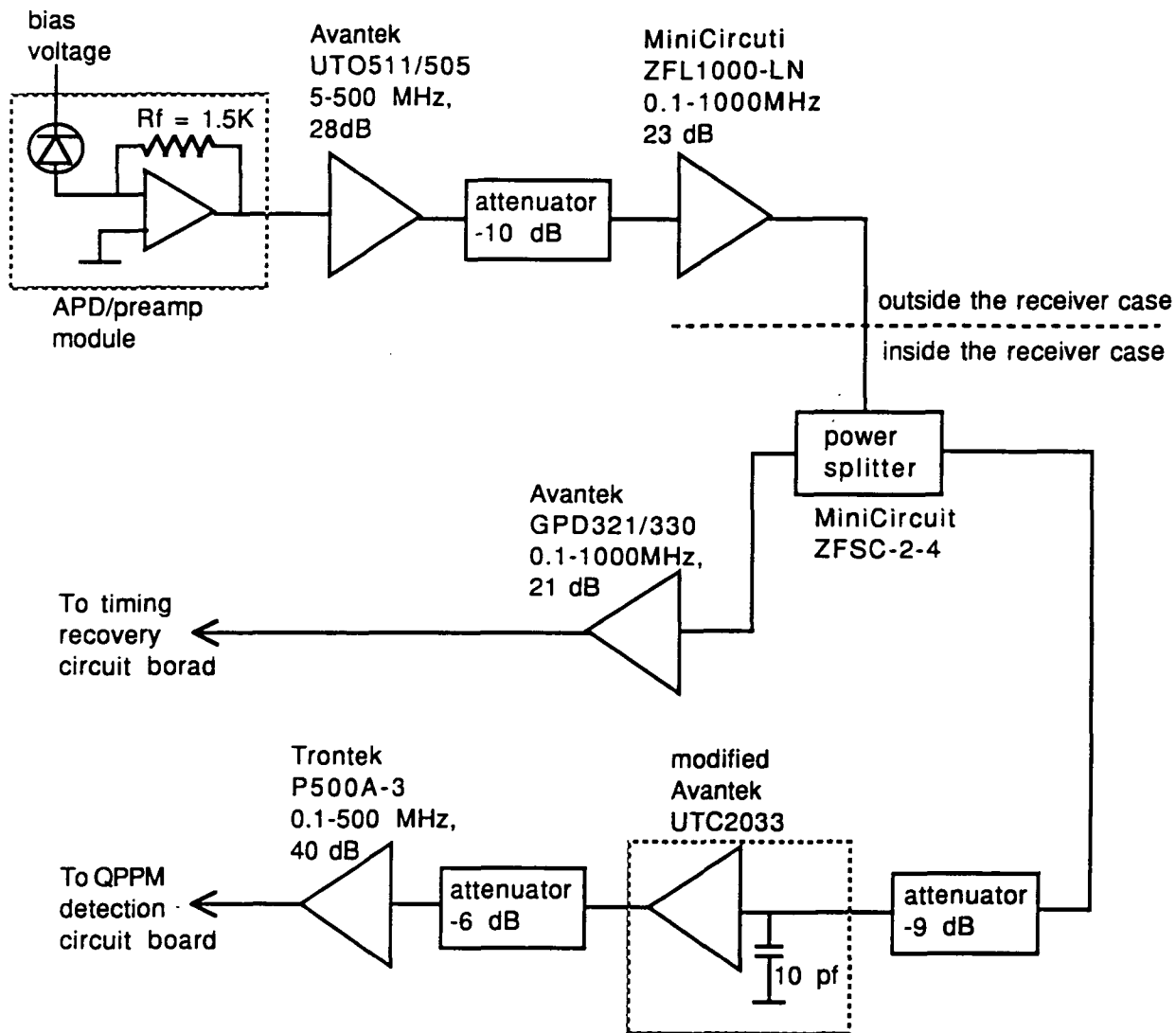


Figure 6. Modified receiver frontend circuit. This should supersede Fig. 4 of Reference [1].

11402 DIGITIZING OSCILLOSCOPE
date: 27-APR-93 time: 11:44:32

{exp:4.1,dig:4.2,dsy:4.0}
Instrument ID# B021597

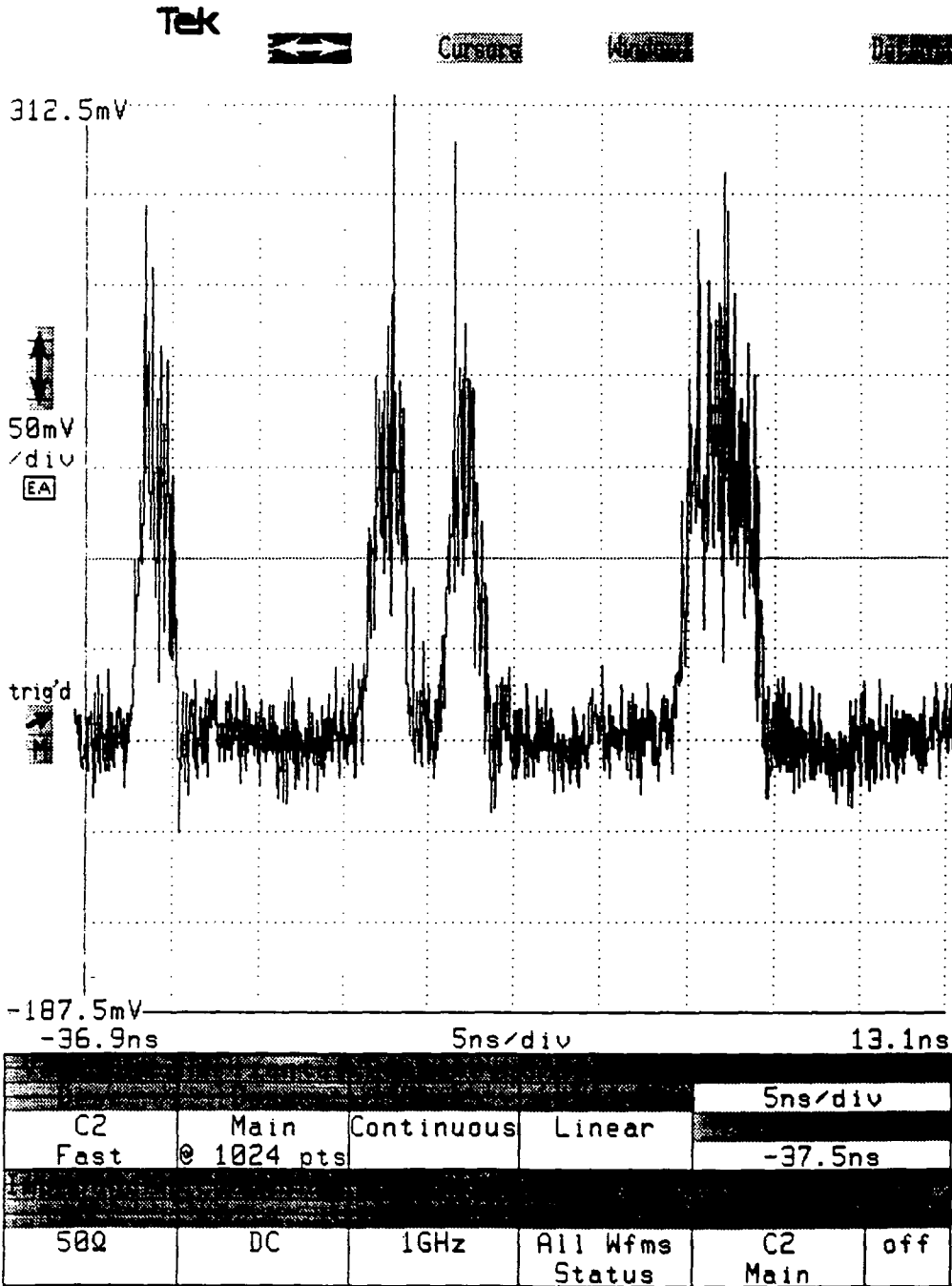
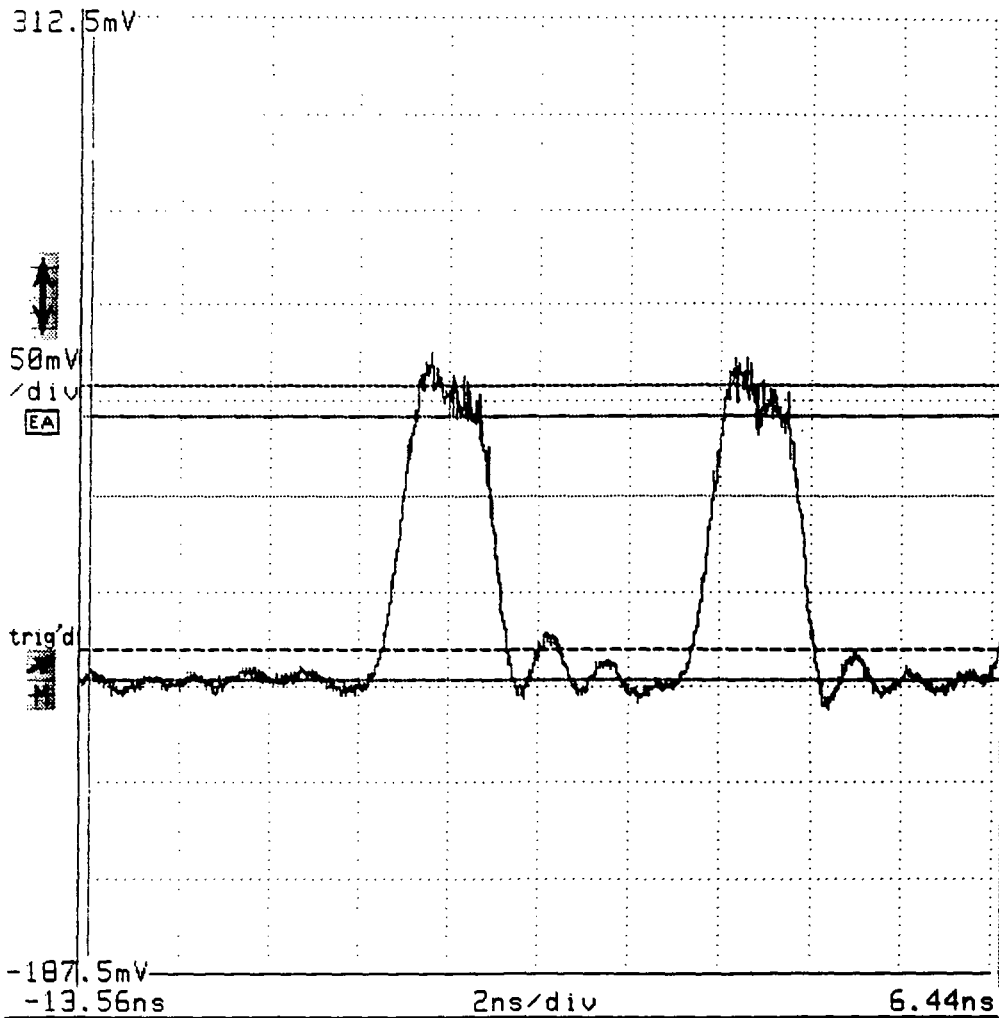


Figure 7. Pulse shapes of input signal to the QPPM receiver.

Tek



-187.5mV		2ns/div		6.44ns	
-13.56ns				120.6mV	
188.4	2.115	728.9		-33mV	
mV	ns	ps			
Fall					
593.1				Avg(C2)	
ps				Main	

Figure 8. Same as Figure 7 but averaged over 64 traces.

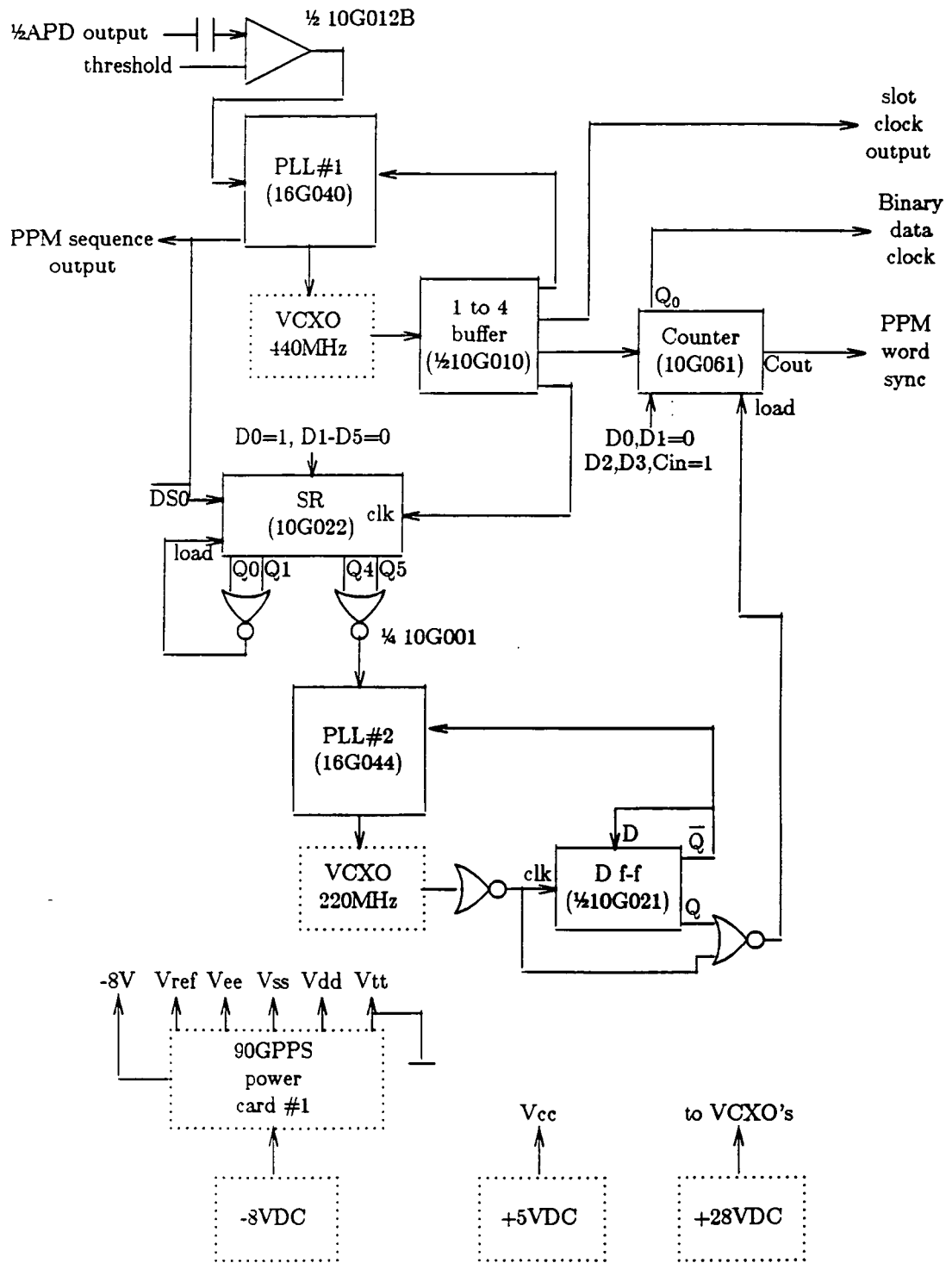
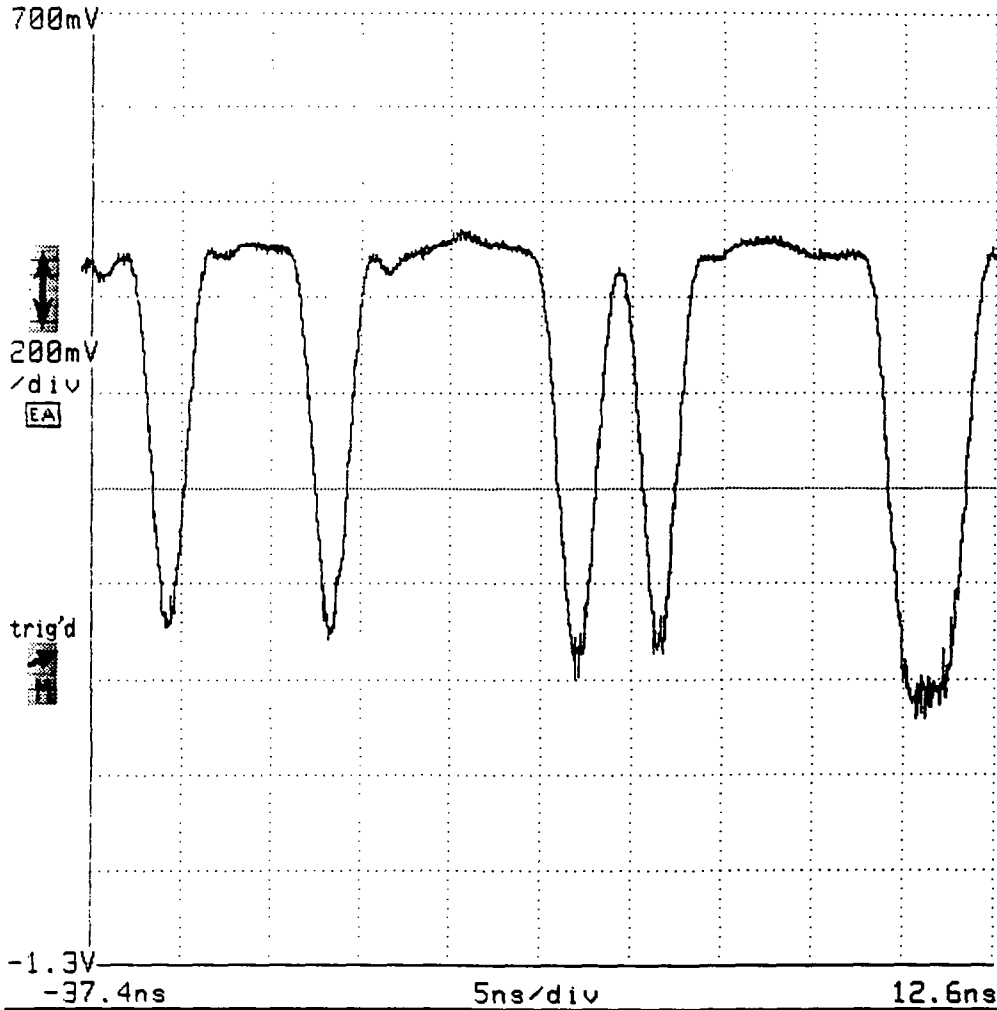


Figure 9. Modified timing recovery circuit (with an additional comparator at the input). This should supersede Fig. 6 of References [1].

Tek



				5ns/div	
Avg(C2)		Main	Avg# >32	Linear	
Fast		@ 1024 pts		-38ns	
I					
50Ω	DC	1GHz	All Wfms Status	Avg(C2) Main	off

Figure 10. Average waveform output from the raised cosine filter (inverting output).

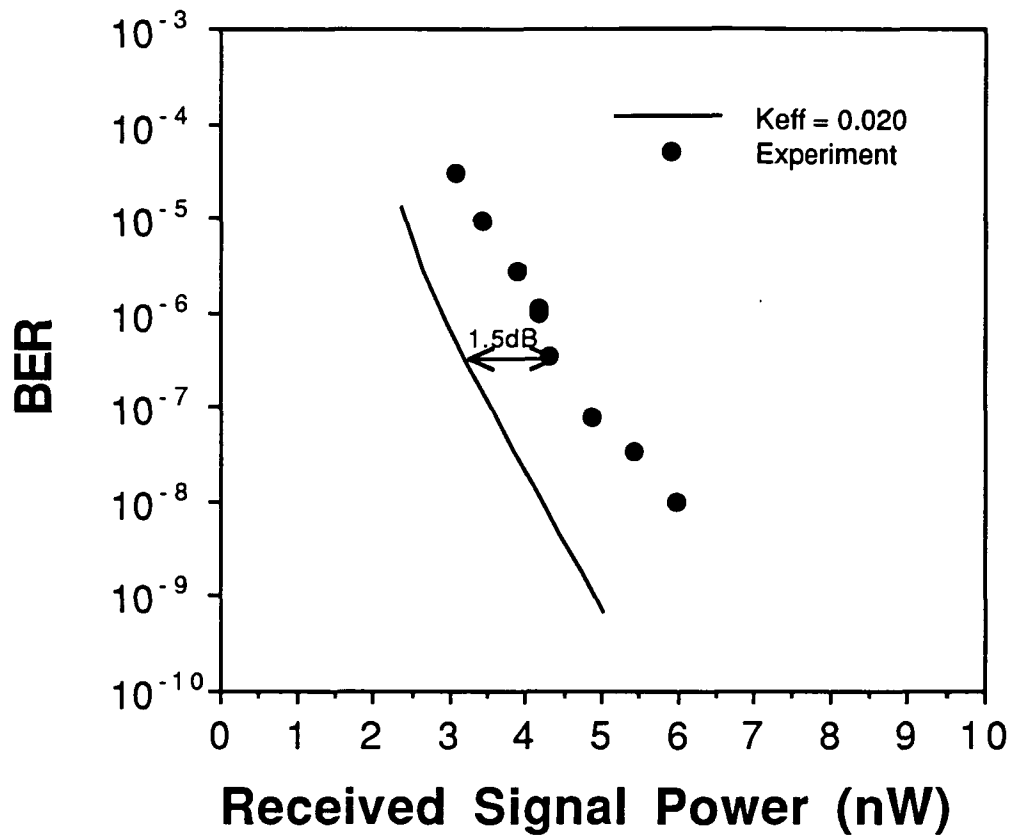


Figure 11. Receiver BER vs. the average received optical signal power. The average APD gain was optimized to $G=110$.